Multivariate geostatistical simulation at Red Dog mine, Alaska, USA

O. Leuangthong, University of Alberta, Edmonton, Alberta,
T. Hodson, Teck Cominco Limited, Vancouver, British Columbia,
P. Rolley, Summit Resources Ltd., Perth, New Zealand, and
C.V. Deutsch, University of Alberta, Edmonton, Alberta

ABSTRACT Red Dog mine is the world's largest Zn producer. The deposit consists of sulphide ore zones in sedimentary exhalative (sedex) deposits and is characterized by the presence of multiple metals and multiple ore types. Existing models considered the multiple elements independently; however, Zn recovery rates were greatly impacted by the percentage of deleterious elements such as Ba and Fe. An exploratory study was initiated to improve the understanding and reproduction of the complex relationships between these key metals. The scope of the case study is to characterize seven different elements, Zn, Pb, Fe, Ba, sPb, Ag, and TOC, within eight different rock types, using a joint simulation approach based on stepwise conditional transformation (SCT).

The transform is a multivariate data transformation technique that partitions the data into several classes and transforms each class to a standard normal distribution. Geostatistical models were constructed for each variable within the eight rock types and subsequently assembled to give 40 realizations for six 7.6 m (25 ft) benches. Gaussian simulation permits reproduction of the input data, original histogram, and variogram of the transformed scores; the benefit of using SCT is that the resulting models also respect multivariate relations locally and globally. This paper documents this case study and key decisions made in the modelling process.

Further, a small synthetic exercise comparing the profit from a kriged and a simulated model is also examined. Results from the exercise show that the simulation approach yielded a 3% increase in profit, relative to the conventional estimation approach.

KEYWORDS Geology, Sulphide, Multivariate simulation, Red Dog

INTRODUCTION

Red Dog mine is located in the DeLong Mountains of the Brooks Range, approximately 90 miles north of Kotzebue, Alaska, United States. The property is owned by the Northwest Alaska Native Association (NANA) Regional Corporation and the mine is operated by Teck Cominco Limited. There are five known deposits in the Red Dog district. Four (Main, Aqqaluk, Paalaaq, and Qanaiyaq) occur in the immediate vicinity of the original discovery, while Anarraaq is approximately 11 km to the north. The deposit consists of sulphide ore zones in sedimentary exhalative (sedex) deposits and is characterized by the presence of multiple metals and multiple ore types. The mine assays for as many as ten variables, the four primary ones being Zn, Pb, Fe, and Ba.

A key issue is the variability within the deposit and the effect this variability has on Zn recovery. Recovery is adversely affected by the presence of high barite and other deleterious minerals and ore textures. The existing long-term resource model was constructed by independently kriging the four main variables. The objective of this study was to apply a geostatistical modelling approach using a multivariate transformation method called the stepwise conditional transformation to jointly model the key elements. Improved multivariate modelling of the different elements and ore types should improve the reliability of the long-term resource model and, therefore, the prediction of Zn recovery.

There are various geostatistical approaches that could be adapted to multivariate data (Journel and Huijbregts, 1978; Wackernagel, 1995; Goovaerts, 1997; Chilès and Delfiner, 1999). Gaussian simulation is common, and the integration of multiple data types could be accommodated by full cosimulation or a simplified collocated cosimulation (Xu et al., 1992). The complex relationships encountered in real data, however, violate the implicit multi-Gaussian assumptions in these approaches and alternative approaches may be required. Direct cosimulation (Soares, 2001) and indicator cosimulation under a Markov-Bayes assumption (Zhu and Journel, 1993) are alternatives to Gaussian-based approaches. Another popular alternative is to consider data transformation for multiple variables such as alternating conditional expectation (ACE; Brieman and Friedman, 1985), principal components analysis (PCA; Goovaerts, 1993), minimum/maximum autocorrelation factors (MAF; Switzer and Green, 1984; Desbarats and Dimitrakopoulos, 2000), and the stepwise conditional transformation (SCT; Leuangthong, 2003; Leuangthong and Deutsch, 2003).

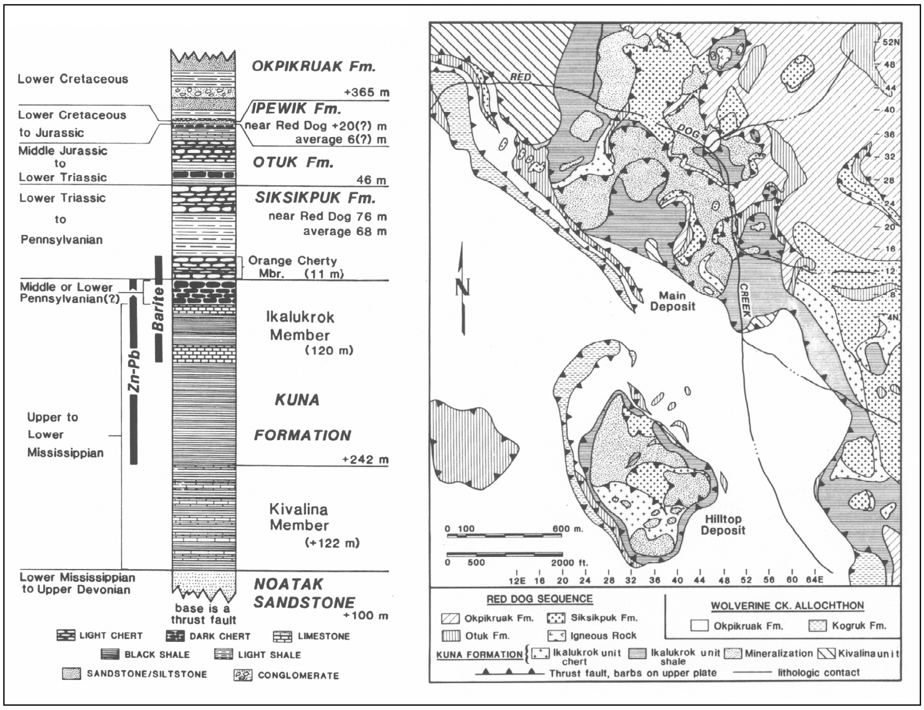

Fig. 1. Stratigraphic section of the Red Dog sequence (left) and bedrock geology for the Main and Qanaiyaq (Hilltop) deposits (right). Source: Moore et al., 1986.

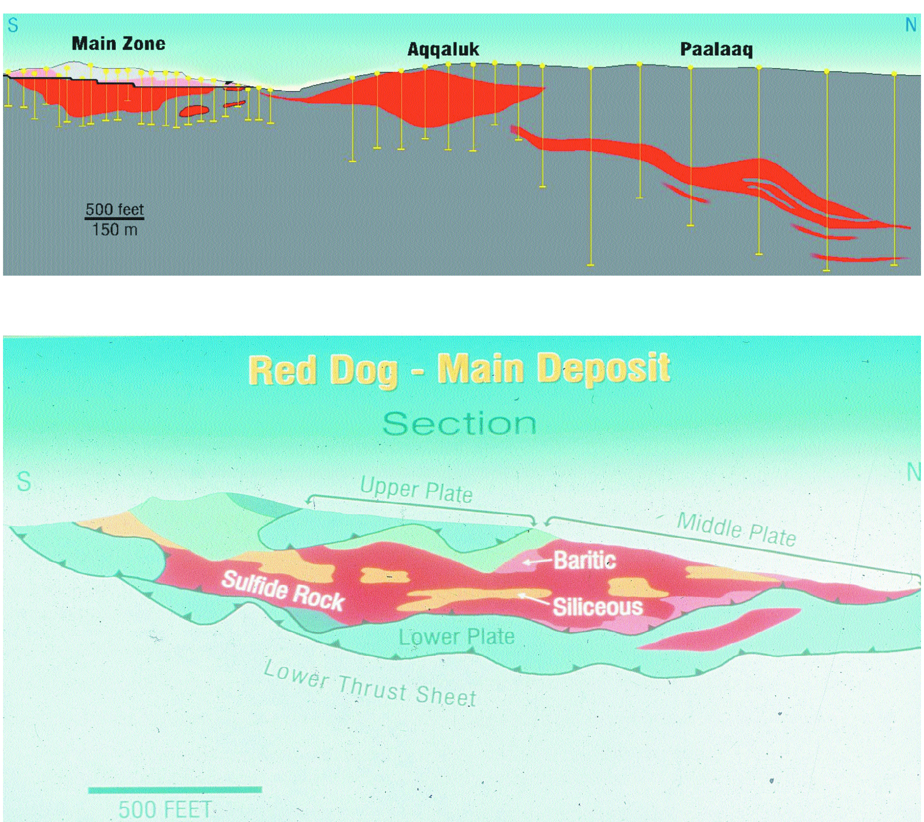

Fig. 2. Idealized section of the Red Dog deposit showing three of the four zones (top) and an idealized section of the Main deposit (bottom).

Despite facilitating the integration and accounting of multivariate data, each transformation approach serves different goals. The aim of ACE is to maximize the linear correlation of the resulting transformed factors, after which conventional Gaussian cosimulation can proceed. PCA aims to decorrelate the data by maximizing the variance of the transformed variables; this may also aid to reduce the dimension of the problem. MAF is an extension of PCA, but applied twice to decorrelate the data at two different lag distances; this yields variables that tend to be spatially uncorrelated. SCT produces Gaussian variables that are uncorrelated; this combination yields transformed variables that are independent at lag **h**=0. All but the latter approach require a second transformation to Gaussianity. With the exception of ACE, all other approaches aim to decorrelate information with the potential benefit of simplifying the problem and the modelling methodology. This paper illustrates the application of the latter transformation approach for simulation of Red Dog's Main pit.

The following sections provide an overview of the geological setting, scope of study, the available data, the simulation approach, and relevant decisions made in the modelling process. This is followed by a small synthetic classification/profit exercise to assess the impact of the proposed methodology and the common independent kriging approach.

OVERVIEW OF GEOLOGY AND AVAILABLE DATA

The Red Dog deposits are sedex, zinc-lead-silver deposits hosted in Mississippian- to Pennsylvanian-age black shale. The deposits are found in the De Long Mountains, which are made up of eight stacked and folded allochthons. The six structurally lowest allochthons are composed of Devonian through to Cretaceous clastic and chemical sedimentary rocks, while the two upper allochthons are of Jurassic and older age and are made of mafic to ultramafic igneous sequences (Moore et al., 1986).

The Red Dog deposits are found in the second lowest allochthon hosted by black siliceous shale and chert of the Ikalukrok unit of the Kuna Formation. The stratigraphic footwall to the mineralization is an interbedded, light gray, calcarenite and dark gray calcareous shale, the Kivalina unit. The deposits themselves are a strata-bound accumulation of siliceous rock, barite, and sulphides. The hanging-wall unit to the mineralization is a silica- and sulphide-poor barite of the lower Siksikpuk Formation of Pennsylvanian to Permian age (Moore et al., 1986). A stratigraphic section and geologic map can be seen in Figure 1.

The Main deposit, as known from drilling and pit mapping, is a nearly flat, elongate stack of mineralized lenses. It extends 1,600 m in a northwest direction, varies in width from 150 m to 975 m, and is up to 135 m thick. The erosion contact of the structural footwall tectonic mélange zone and underlying Okpikruak formation of the Wolverine Creek allochthon forms the western and southwestern edge of the deposit. To the north and northeast, the Main merges with the Aqqaluk deposit. Main and Aqqaluk are actually one deposit separated for reserve purposes along a boundary defined by the Red Dog and Shelly Creek diversions.

The Main deposit consists of two major and one minor mineralized plates and their associated overlying waste rocks. The upper plate is a flat-lying sheet of Kivalina unit limestone and shale, Ikalukrok unit siliceous shale, and sulphide-bearing barite rock. The median plate contains most of the reserves in the Main zone and consists of a sequence of massive to semi-massive sulphide rock, sulphide-bearing silica rock, and sulphide-bearing barite rock. The mineralized portion of the median plate is capped with a sequence of shale and chert of Siksikpuk, Otuk, and Okpikruak units. The lower plate mineralization in the Main deposit consists of sulphide-veined, silicified, Ikalukrok shale, semi-massive to massive sulphides, and sulphide-bearing barite rock. An idealized south to north section through the Main deposit is shown in Figure 2.

The scope of this case study is limited to eight geological rock types corresponding to four different ore type units in the Upper and Median plates. These were chosen because they correspond to a volume that includes both recently mined material and material that will be mined in the near future.

The existing grade models were independently kriged at a 7.6 m by 7.6 m by 7.6 m (25 ft by 25 ft by 25 ft) resolution. The geostatistical models will be simulated at 3.8 m by 3.8 m by 3.8 m (12.5 ft by 12.5 ft by 12.5 ft) resolution, and later upscaled to 7.6 m (25 ft) cubed for comparison purposes. There are some good reasons to model at a finer scale than is required. Firstly, the 3.8 m (12.5 ft) composite data are a good compromise between retaining some of the variability of the smaller drillhole sample data and the faster simulation of larger and, hence, fewer cells. Secondly, the simulation is essentially a "point"-scale simulation; current implementations of Gaussian simulation do not explicitly account for volume-variance relations. Thus, simulating at a finer resolution and then averaging to larger blocks shows the variability of the block grades more accurately.

Six benches will be modelled, spanning a volume that is 1370 m (4,500 ft) wide (easting) by 1370 m (4,500 ft) long (northing) by 46 m (150 ft) vertical span (elevation). The model will consist of a total of 1,555,200 grid points. The simulations will be constructed on a by rock type basis and all figures shown will correspond to one particular rock type. Once all rock types are simulated, the realizations will be merged. All global comparisons consist of all rock types taken together.

Three types of data were available: drillhole data, composited drillhole data, and blasthole data. Multivariate geostatistical modelling considered the 3.8 m (12.5 ft) composites. A geology model at 7.6 m (25 ft) resolution was also available. For consistency with the simulation models, the 7.6 m (25 ft) geology block model was reformatted into a 3.8 m (12.5 ft) block model.

There were a total of 9,847 3.8 m (12.5 ft) composites available for the eight rock types of interest. The term drillhole (DH) refers to the 3.8 m (12.5 ft) composites. DH data are at a nominal 30 m by 30 m (100 ft by 100 ft) spacing. For these same rock types, there were 58,566 blasthole (BH) data available for model validation. BH data are more closely spaced than DH data at 3 m by 3.7 m (10 ft by 12 ft) spacing with 7.6 m (25 ft) vertical extent (the vertical span is one bench). Figure 3 shows the projection of the available DH data onto the horizontal and vertical plane.

MULTIVARIATE SIMULATION APPROACH

Conditional simulations were performed for seven variables: Zn, Pb, Fe, Ba, sPb (soluble Pb), Ag, and TOC (total organic content). These seven variables were modelled for each rock type, using Gaussian simulation with stepwise conditionally transformed (Leuangthong, 2003) variables. The main steps of the simulation are:

1. Data declustering to obtain representative distributions for each variable.
2. Transforming data in a stepwise conditional (Rosenblatt, 1952; Luster, 1985; Leuangthong and Deutsch, 2003) manner to obtain independent Gaussian variables.
3. Calculating and modelling the directional variograms for each of the transformed variables within each rock type.
4. Independently simulating transformed variables via sequential Gaussian simulation (Isaaks, 1990).
5. Back transforming simulated values in a stepwise conditional manner to return values to original units.
6. Validating simulation results to confirm data, histogram, crossplot, and variogram reproduction.

Once all variables within all rock types were modelled, the block models were merged to form multiple realizations of the study area for uncertainty assessment and post-processing. All simulation-related tasks were performed using GSLIB (Deutsch and Journel, 1998) and other GSLIB-compatible tools.

The proposed methodology is a fairly common approach to geostatistical Gaussian simulation; the main difference is the use of the stepwise conditional transformation (SCT) in place of the conventional normal score transform. SCT is a multivariate Gaussian transformation approach whereby the primary variable is transformed to be standard normal, and all subsequent variables are successively conditioned to the previous variable(s) based on probability binning (Rosenblatt, 1952; Luster, 1985; Leuangthong, 2003). A simple numerical example of how the transform is actually performed is illustrated in Figure 4.

The transform applies to collocated multivariate data and facilitates multivariate modelling by removing complex dependencies between the variables, making them independent, prior to simulation. Cross variograms between transformed variables should be checked to verify that spatial correlations are approximately zero. After such verification, independent Gaussian simulation can proceed. Back transformation restores the complex relationships between the multivariate data.

The need to consider seven variables simultaneously for any one rock type poses a problem in practice; this is the case for Red Dog. The multivariate stepwise conditional transform would require 10^7 composites in order to have a minimum of ten data per probability class. This is impractical. A nested application of the stepwise conditional transformation is proposed to overcome this problem. Accounting for a lower-dimensional multivariate distribution was considered. Inference of a trivariate distribution would require approximately 10^3 or 1,000 data to define the conditional distributions with a minimum of ten data. This is more reasonable, given the number of composites available.

The transformation ordering for the stepwise conditional transform will affect the reproduction of the variogram from simulation. Thus, the most important variable or the most continuous variable should be chosen as the primary variable (Leuangthong and Deutsch, 2003). For Red Dog, Zn is the most important variable, and so all others will be conditioned to it. To account for the other six variables, sets of transformations were proposed (Table 1).

The transformation order reflects the significance Teck Cominco staff attribute to each variable. Zn was considered to be the most important, and so all other variables were transformed conditional to Zn. In all cases, Fe or Pb act as secondary variables, and all remaining variables were then transformed conditional to either Zn and Pb or Zn and Fe. The choice of the secondary variable in each transform order reflects the relationship between the secondary and tertiary variable; however, this cannot be measured by the correlation coefficient alone as the correlation summarizes only the linearity of this relationship. Non-linearities and constraint features (if present) would not be captured by this statistic; an examination of crossplots between the different elements can easily reveal any complex relationships. In all cases, the determination of the secondary variable was based on careful assessment of the relevant bivariate and trivariate distributions.

Declustering was performed to assemble representative distributions for each variable. Given the multivariate nature of this dataset and the intended application of a multivariate transformation technique, declustering must be consistent between all variables. Although the location map of drillholes (Fig. 3) shows a fairly regular grid of data, it must be noted that data across all rock types are shown; declustering must be performed within rock types, across geological boundaries (based on an available geology model, which results in irregular data spacing). The representative distribution of Zn was obtained by using the accumulated weights obtained from kriging within a rock type; this approach not only respects the rock type being populated, but it also respects the spatial variability of the data and hence their area of influence within this rock type.

Secondary variables (say Pb) were declustered through a bivariate calibration of the Pb distribution using both the representative distribution of Zn and the crossplot of Zn and Pb. Specifically, the representative distribution of Zn is divided into a series of classes and the corresponding conditional distributions of Pb are determined. The representative distribution of Pb is

Table 1. Transformation ordering for stepwise conditional transformation

Transform No.	Variable	Conditioning Variable(s)
1	Zn	
2	Pb	Zn
3	Fe	Zn, Pb
4	Ba	Zn, Fe
5	sPb	Zn, Pb
6	Ag	Zn, Pb
7	TOC	Zn, Fe

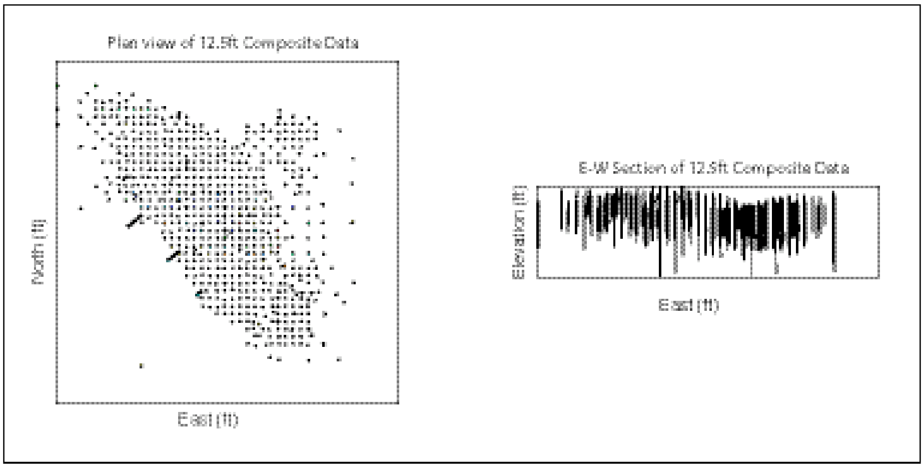

Fig. 3. All available drillhole data projected onto a horizontal plane (plan view, left) and onto a vertical plane (E-W sectional view, right).

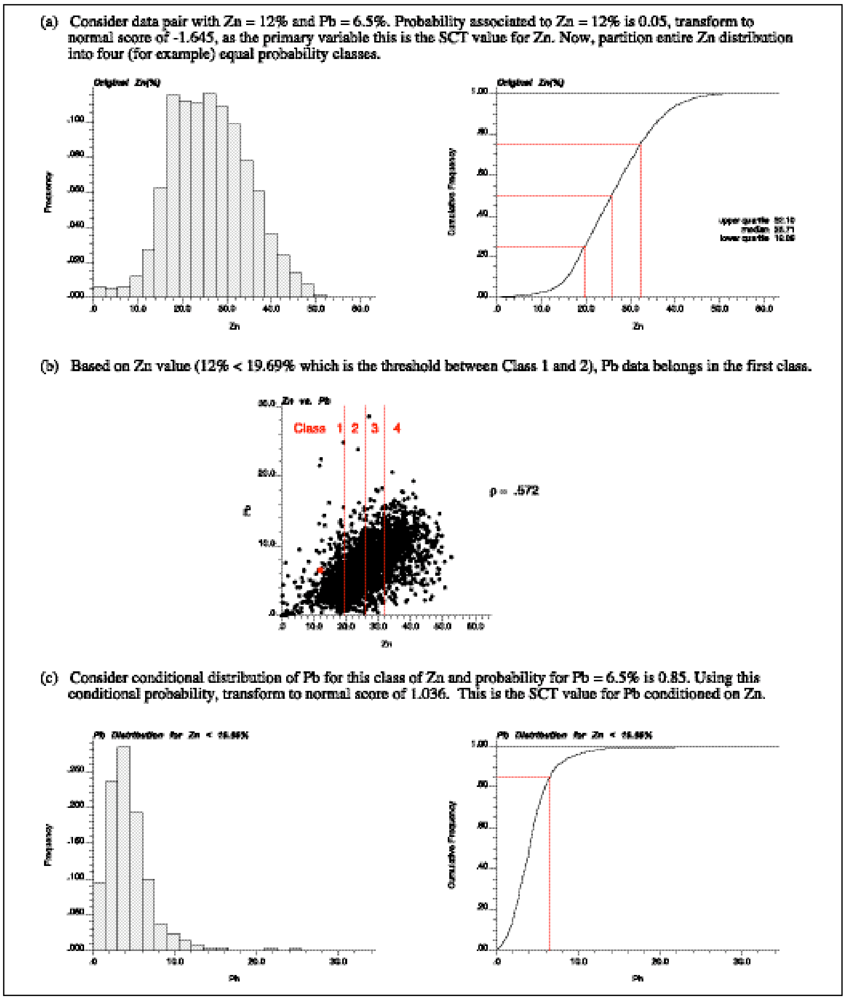

Fig. 4. Numerical example of SCT for two variables, Zn and Pb: a) transformation of the primary variable, Zn; b) determination of corresponding conditional distribution for the secondary variable, Pb; and c) transformation of Pb using the conditional distribution determined based on paired Zn value. Only those statistics and plots relevant to the transform are shown.

then constructed by accumulating all of the conditional distributions weighted by the representative probability of Zn for the corresponding class (Figure 5). For all tertiary variables, the same rationale was applicable, and the representative histograms for Fe through TOC were determined using the representative histograms for the two dependent variables plus the trivariate calibration data.

Stepwise conditional transformation was then performed on these representative distributions. Figure 6 shows the scatterplots of the variables resulting from the first transform sequence of Zn, Pb, and Fe (Table 1). The transformed variables are independent and multi-Gaussian, which translates to a circular shape in the crossplot. From Figure 6, the crossplot between the first two variables (Zn and Pb) appears approximately circular. Crossplots with the third variable (Fe, in this case) show some banding; however, this is simply a numerical artefact of having many classes and, consequently, fewer data within each class (Leuangthong, 2003). This banding does not impact data reproduction. Independence of the transformed variables means that each variable can be simulated independently.

Variograms were then calculated and modelled for each of the transformed variables. Figure 7 shows an example of the horizontal and vertical variogram models for the stepwise conditionally transformed Zn, Pb, Fe, and Ba for one rock type. Note that secondary and tertiary variables exhibit a relatively high nugget effect; because the transform imposes independence for collocated data by transforming each class separately, a high nugget effect of subsequently transformed variables is understandable (Leuangthong and Deutsch, 2003). Further, cross variograms were calculated and checked to confirm approximately zero correlation for all lag distances.

Sequential Gaussian simulation was independently performed for the seven transformed variables on a by rock type basis. A total of 40 realizations were generated for each variable within each rock type. For greater computational efficiency, only those blocks belonging to the specific rock type were simulated. Each realization was then back transformed to the original units of the data. Similar to the forward transformation that relied on

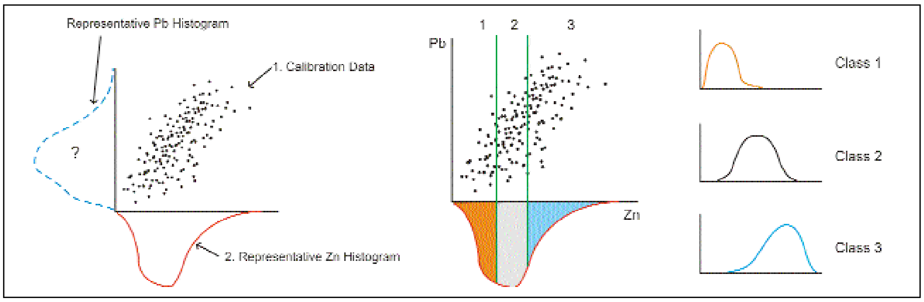

Fig. 5. Schematic illustration showing multivariate calibration data, representative Zn histogram and representative Pb histogram to be determined (left); division of multivariate calibration data into multiple classes, with distributions on the right representing the conditional distribution of Pb for each class (right). Weights applied to conditional Pb distribution all shown in light blue, gray, and orange shaded regions of Zn histogram.

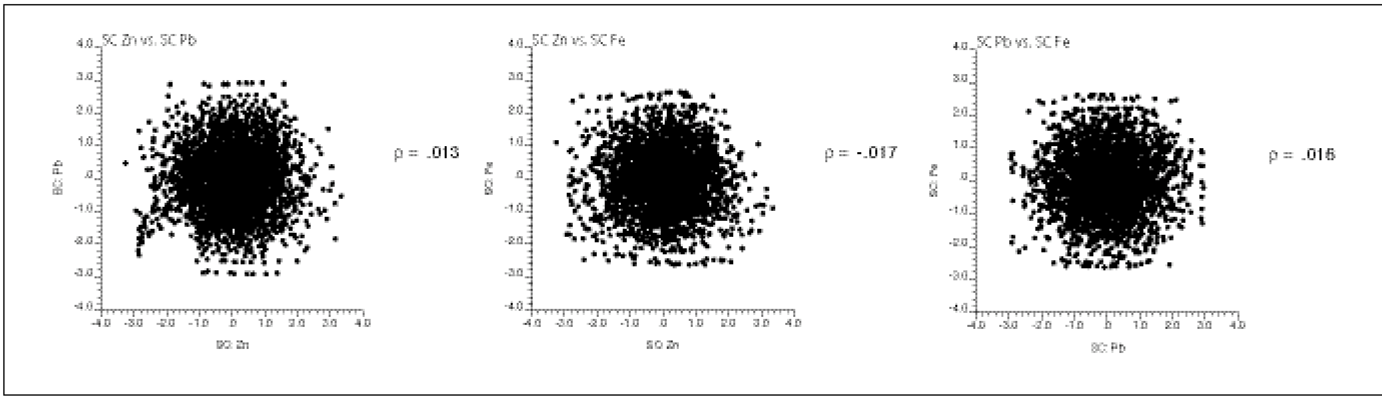

Fig. 6. Crossplot between stepwise conditionally transformed variables for Zn, Pb, and Fe. Zn was transformed first, then Pb was transformed conditional to Zn, and finally Fe was transformed conditional to both Zn and Pb.

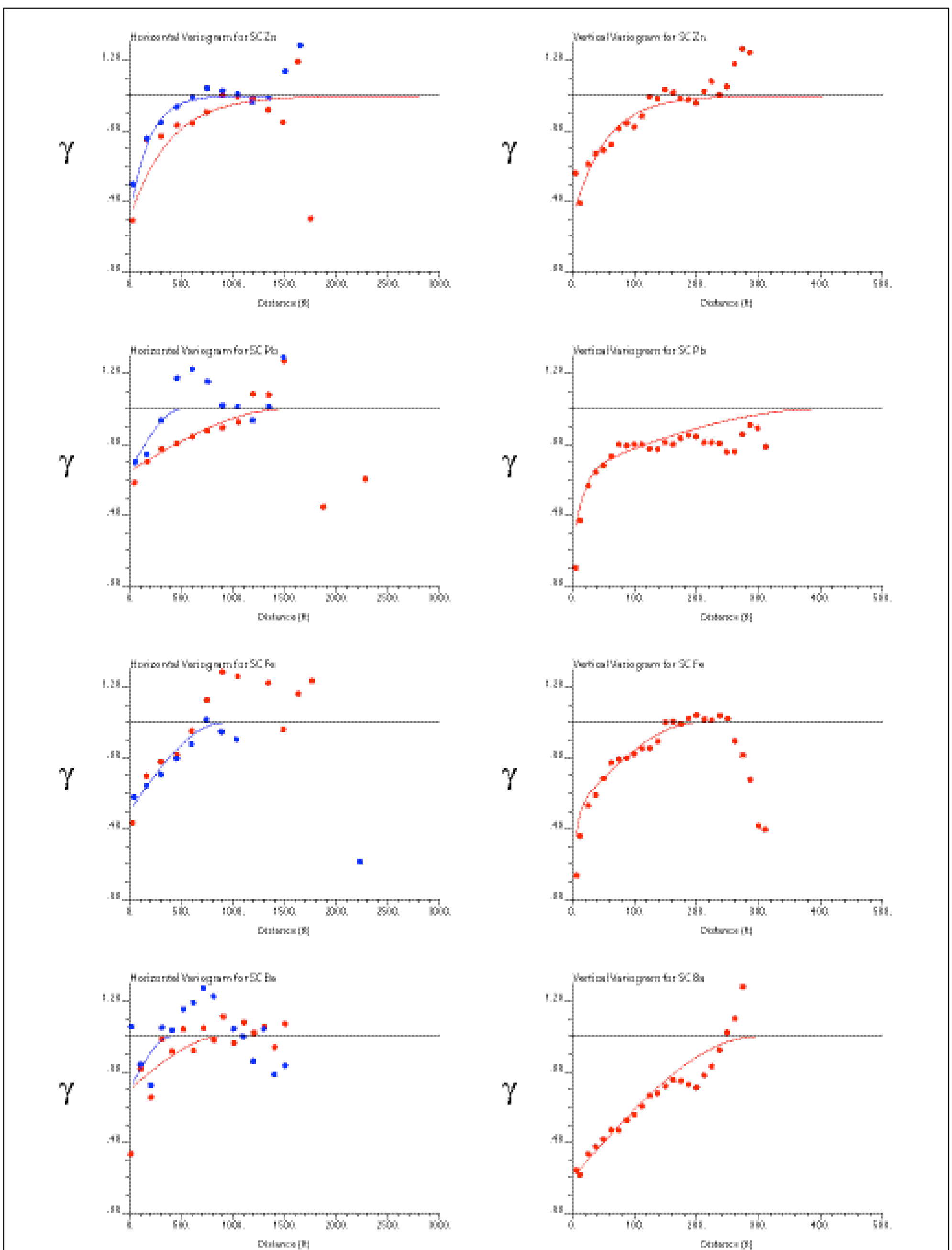

Fig. 7. Horizontal (left) and vertical (right) variograms for stepwise conditionally transformed Zn, Pb, Fe, and Ba for one rock type.

conditioning one variable to another, the back transformation for each simulated realization must be performed in a conditional fashion. For example, the back transform of Fe is conditional to the simulated values for Zn and Pb.

The simulations were thoroughly checked to ensure reproduction of (1) the composite values at their respective locations, (2) the histogram and associated summary statistics, and (3) the variograms in Gaussian space of the stepwise transform scores. Reproduction of these three statistics is not unexpected, as the theoretical development of Gaussian simulation is formed on this very basis (Journel, 1989). For this multivariate simulation, the multivariate relations were also checked. The simulated models were upscaled to 7.6 m by 7.6 m by 7.6 m (25 ft by 25 ft by 25 ft) blocks to facilitate comparisons with the 7.6 m (25 ft) composites and also the existing long-term model.

Figure 8 shows a comparison of the crossplot reproduction from simulation to those crossplots from the 7.6 m (25 ft) composites and the existing long-term resource model. In general, the simulated realizations reproduce the trivariate relations with comparable variability to the 7.6 m (25 ft) composites; the corresponding plots from the existing long-term model shows similar bivariate relations, but with noticeably reduced variability. Recall that it is this variability between the multiple elements that was impacting the Zn recovery and provided the motiva-

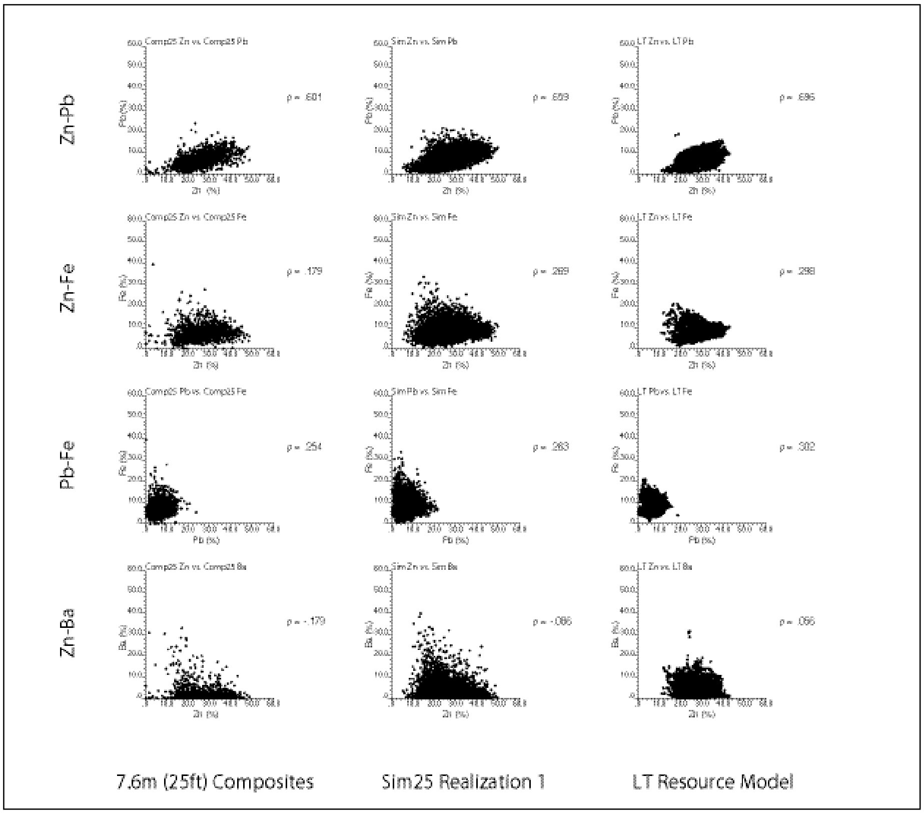

Fig. 8. Comparison of multivariate features reproduction for Zn-Pb (top row), Zn-Fe (second row), Pb-Fe (third row), and Zn-Ba (bottom row). Cross-plots using the 7.6 m (25 ft) composites are shown on the left column, from the upscaled simulations are shown in the middle, and from the available long-term resource model are shown in the right column.

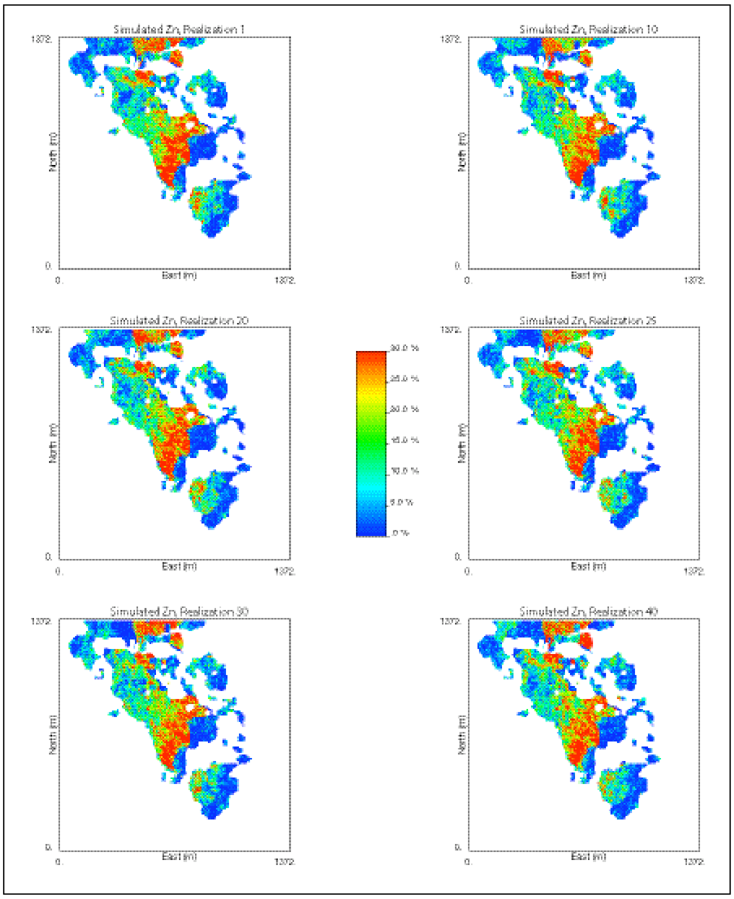

Fig. 9. Simulated realizations of Zn at 3.8 m (12.5 ft) grid resolution.

tion to undertake such a case study.

Once all simulated models were generated and validated on a by rock type basis, a single realization for each variable was obtained by merging the simulated properties from each rock type. With these multiple realizations (Figure 9), the uncertainty at any location and/or region can be assessed.

COMPARISON OF PROFIT EXERCISE

In practice, multiple variables are estimated independently with ordinary kriging. This section addresses the impact of the multivariate simulation approach using the stepwise conditional transform relative to the conventional practice of kriging. Note that this exercise is for illustrative purposes only; prices and recovery functions have been synthetically developed and greatly simplified for this specific exercise.

The idea is to compare the profit of ore from both methods with true reference data coming from Red Dog. A profit function is applied to obtain a true profit dataset. A subset of the reference data will be extracted and used to model the grades using both kriging and simulation. The profit function will be applied to these grade models. Based on the expected profit from each approach, each location within the model will be classified as either ore or waste. The true profit at each location is known, so the profit from each model can be calculated.

PROFIT FUNCTION

The real profit function was not available; a simple profit function was developed to account for Zn and Pb grades, recovery functions, and metal prices. At the time of this work, Teck Cominco was developing new functions based on extensive metallurgical testing to reflect the impact of Ba on Zn recovery. In light of this activity and given that the presence of contaminants such as Ba and Fe would affect Zn recovery, penalty functions to account for this impact were considered. The Pb recovery is constant.

The constructed models provide the metal grades. All other parameters were developed or chosen to be constant. The metal recoveries for both Zn and Pb were calculated as Red Dog's five-year average recovery (1998-2002), based on Teck Cominco's financial report (Teck Cominco, 2003). These were 83.6% Zn recovery and 58.7% Pb recovery. The penalty functions, constructed to mimic the impact of Fe and Ba on Zn recovery (decreasing functions on a scale of 0 to 1.0), were used to determine a multiplicative factor for the maximum Zn recovery of 83.6%; in this way, high Fe or Ba content would result in reduced Zn recovery. The price for Zn was chosen to be $680/ton of Zn, and the price for Pb was chosen as $380/ton of Pb; both prices were approximated based on the metal prices from the London Metal Exchange in 2003. In order to yield approximately 50% ore and 50% waste classification, the cost per ton mined was chosen arbitrarily.

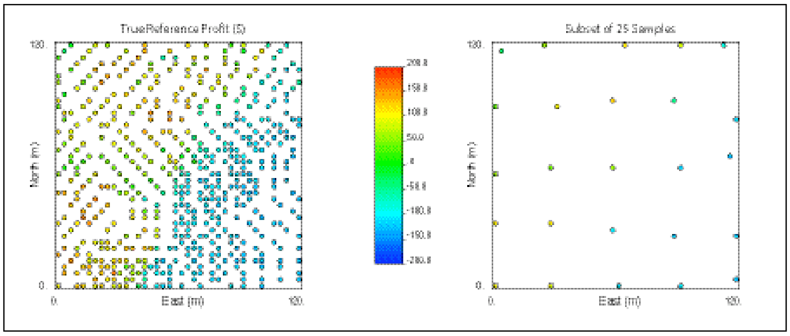

Fig. 10. Location map of reference BH data (left) and sampled BH data (right) for use in comparing model approaches.

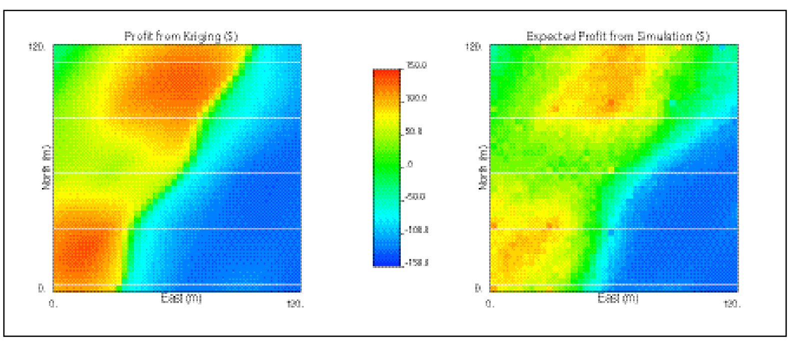

Fig. 11. Comparison of profit map for ore/waste classification from kriging (left) and simulation (right).

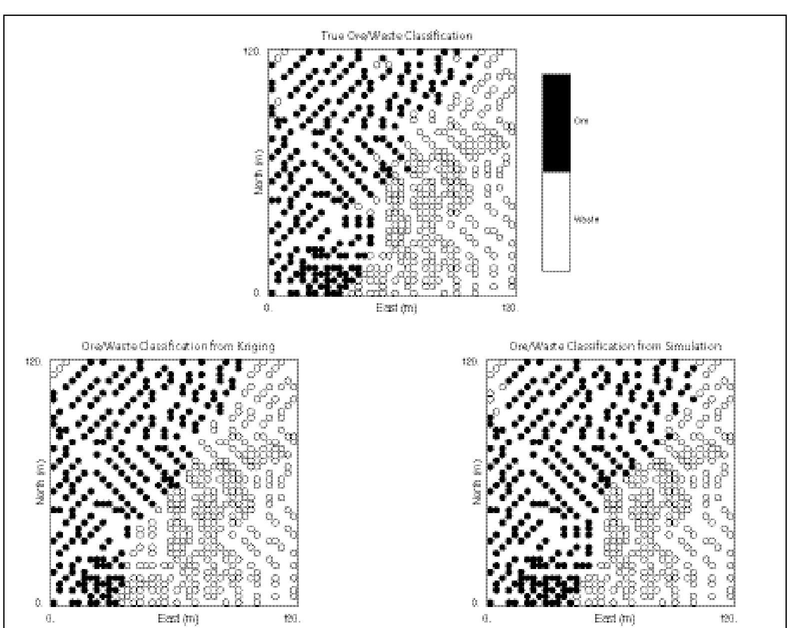

Fig. 12. Comparison of true ore/waste classification (top) and the classification from kriging (bottom left) and simulation (bottom right) at data locations.

REFERENCE DATA

For a fair comparison to be made, real data must be used. The density and number of BH data available make it an attractive database as a reference data set. Rather than modelling the entire area, only a small area was modelled. The area was chosen to be in a marginal zone, where ore/waste classification based on the models would have the largest impact.

Figure 10 shows the available BH data in the chosen region of 120 m by 120 m (400 ft by 400 ft) in the 850 bench, and the subset of data extracted from this region. The available data consists of 532 BH samples of Zn, Pb, Fe and Ba. From this dataset, 25 samples separated at a nominal 30 m by 30 m (100 ft by 100 ft) spacing were chosen to act as exploration data. This spacing is consistent with the DH data available for Red Dog. This subset of data was used as conditioning data for kriging and simulation.

MODEL CONSTRUCTION

The model grid was chosen to be 3 m by 3 m by 7.6 m (10 ft by 10 ft by 25 ft), which is similar to the 3 m by 3.7 m by 7.6 m (10 ft by 12 ft by 25 ft) spacing of the BH data. A total of 1,600 grid points were modelled. Further, variograms for both approaches were calculated and fitted using the reference 532 BH data. This filtered out the influence of poor variogram inference due to scarce data.

The variograms for kriging were calculated for the original data, and the variograms for simulation were calculated and fitted for the stepwise conditionally transformed data. In both sets of variograms, a trend was apparent from the experimental points extending beyond the sill of 1.0. This was not surprising given that the area was purposely chosen to be in the transition zone between ore and waste; hence, a trend from low to high grades was expected. Trend modelling was not performed for this exercise because of the relatively small area.

For kriging, each variable was estimated independently using ordinary kriging. For simulation, the stepwise conditionally transformed variables were independently simulated using sequential Gaussian simulation to generate 100 realizations of the grades and subsequently back transformed to the original units of the data.

RESULTS

These grade models were then processed by applying the profit function at each location within the model. Although 100 realizations of profit were available from simulation, the ore/waste classification was based on the expected profit map obtained by calculating the expected value of profit at each location. Figure11 shows the profit map obtained from simulation and kriging.

Although 1,600 locations were modelled, only the 532 points corresponding to locations where true data were available can be compared. At these locations, the true profit was known. The profit model from kriging and expected profit model from simulation were used to classify the 532 locations as either ore or waste. Figure 12 shows the comparison of the ore/waste classification of the 532 locations from the true reference data to the kriging and the simulation approaches. Overall, both approaches clearly show the waste and ore regions; relatively few blocks were misclassified.

Table 2 shows the summary of the ore/waste classification from both kriging and simulation relative to the true classification. The tables show that the kriging approach resulted in a total 7% of blocks that were misclassified, compared to the 6% misclassified by simulation. From the true profit, 251 blocks (47% of the true data) were classified as ore; simulation correctly classified ore for 98% of those blocks, while kriging correctly classified 90% of those blocks.

Table 2. Ore/waste classification summary of kriging (left) and simulation (right) relative to true ore/waste classification. The top row shows the number of locations classified, while the bottom row shows the percentage of locations classified relative to the true classifications given by the totals listed in the top tables.

		True				True	
		Ore	**Waste**			**Ore**	**Waste**
Kriging	Ore	225	11	Simulation	Ore	246	27
	Waste	26	270		Waste	5	254
	Total	251	281		Total	251	281

		True				True	
		Ore	**Waste**			**Ore**	**Waste**
Kriging	Ore	90%	4%	Simulation	Ore	98%	10%
	Waste	10%	96%		Waste	2%	90%

For those blocks classified as ore, the profit of ore mined as a result of the classification from each method was compared with the true profit of $7.89 million. The results from such a comparison showed that the simulation approach yielded $7.28 million, while kriging yielded $7.06 million in profit. Although these profit values appear high for the relatively small area of a single bench, the relative percentage increase in profit is the key result. Multivariate simulation resulted in 92% of the true profit relative to the 89% yielded by kriging. In practice, this 3% difference may translate to several millions of dollars in increased profit if a larger area and multiple benches are considered.

CONCLUSIONS

For the seven variables within the eight rock types, conditional simulation models were constructed using the stepwise conditional transformation technique to account for the multivariate relations. These models were developed using 3.8 m (12.5 ft) composites and a geology model at 7.6 m (25 ft) resolution. Each model was validated by checking reproduction of the input drillhole data, representative histogram, variogram, and the multivariate distributions.

Conventional Gaussian cosimulation approaches are sufficient for straightforward multivariate problems; however, for the complexity of the Red Dog deposit, these common approaches are inadequate. The availability of multiple metal grades within multiple rock types warrants some consideration of the relationship between these grades, and how these relationships change from one rock type to the next. The approach documented in this paper was designed to explicitly address this key issue. Consequently, the resulting models not only reproduce the univariate data and its spatial variability, but taken together, they also honour the multivariate relations between the different metals/minerals within the different rock types.

A comparison of the multivariate simulation approach used in this case study and the common practice of kriging multiple variables independently showed that the simulation models resulted in an increase in profit of 3% over the kriging approach, yielding a total of 92% of the true profit.

ACKNOWLEDGMENTS

The authors would like to acknowledge the industry sponsors of the Centre for Computational Geostatistics (CCG) at the University of Alberta for supporting this research. In particular, we wish to thank Teck Cominco Limited for allowing the publication of this case study and their continued support of the CCG.

Further, the reviewers are thanked for their time and effort in reviewing the original manuscript. Their constructive comments and suggestions towards improving this paper are gratefully appreciated.

Paper reviewed and approved by the Geological Society of CIM.

Oy Leuangthong is an assistant professor in the School of Mining and Petroleum Engineering at the University of Alberta. She is an Alberta Ingenuity Researcher, and teaches and conducts

research into improved characterization of natural resources using geostatistics.

Terry Hodson is employed with Teck Cominco Ltd. as assistant manager, resource evaluation. He has 25 years of exploration, mine operations, and resource evaluation experience in the mining industry. He holds a B.Sc. degree (honours) in geology from the University of British Columbia.

Peter Rolley is a geologist with 25 years of exploration, resource estimation, and mine development experience in the Australasian and international mining industry. He holds a B.Sc. degree (honours) in geology from the University of Melbourne and an M.Sc. in economic geology from the University of Queensland.

Clayton V. Deutsch holds the Canada Research Chair in Natural Resources Uncertainty Characterization and the Alberta Chamber of Resources Industry Chair in Mining Engineering. He is director of the School of Mining and Petroleum Engineering at the University of Alberta. He teaches and conducts research into better ways to model heterogeneity and uncertainty in mineral deposits.

REFERENCES

BRIEMAN, L. and FRIEDMAN, J., 1985. Estimating optimal transformations for multiple regression and correlation. Journal of the American Statistical Association, 80, p. 580-598.

CHILÈS, J.P. and DELFINER, P., 1999. Geostatistics: Modelling Spatial Uncertainty. John Wiley & Sons Inc., New York, 695 p.

DESBARATS, A.J. and DIMITRAKOPOULOS, R., 2000. Geostatistical simulation of regionalized pore-size distributions using min/max autocorrelation factors. Mathematical Geology, 32, p. 919-942.

DEUTSCH, C.V. and JOURNEL, A.G., 1998. GSLIB: Geostatistical Software Library and User's Guide, 2nd Edition. Oxford University Press, New York, 369 p.

GOOVAERTS, P., 1993. Spatial orthogonality of the principal components computed from coregionalized variables. Mathematical Geology, 25, p. 281-302.

GOOVAERTS, P., 1997. Geostatistics for Natural Resources Evaluation. Oxford University Press, New York, 483 p.

ISAAKS, E.H., 1990. The Application of Monte Carlo Methods to the Analysis of Spatially Correlated Data. Ph.D. thesis, Department of Applied Earth Sciences, Stanford University, Stanford, California, 213 p.

JOURNEL, A.G., 1989. Fundamentals of Geostatistics in Five Lessons. Short Course in Geology, American Geophysical Union, Washington, District of Columbia, 8, 40 p.

JOURNEL, A.G. and HUIJBREGTS, C.J., 1978. Mining Geostatistics. Academic Press, London, 600 p.

LEUANGTHONG, O., 2003. Stepwise Conditional Transformation for Multivariate Geostatistical Simulation. Ph.D. thesis, Department of Civil and Environmental Engineering, University of Alberta, Edmonton, Alberta, 192 p.

LEUANGTHONG, O. and DEUTSCH, C.V., 2003. Stepwise conditional transformation for simulation of multiple variables. Mathematical Geology, 35, p. 155-173.

LUSTER, G.R., 1985. Raw Materials for Portland Cement: Applications of Conditional Simulation of Coregionalization. Ph.D. thesis, Department of Applied Earth Sciences, Stanford University, California, 531 p.

MOORE, D.W., YOUNG, L.E., MODENE, J.S., and PLAHUTA, J.T., 1986. Geologic setting and genesis of the Red Dog zinc-lead-silver deposit, Western Brooks Range, Alaska. Economic Geology, 81, p. 1696-1727.

ROSENBLATT, M., 1952. Remarks on a multivariate transformation. Annals of Mathematical Statistics, 23, 3, p. 470-472.

SOARES, A., 2001. Direct sequential simulation and cosimulation. Mathematical Geology, 33, p. 911-926.

SWITZER, P. and GREEN, A.A., 1984. Min/Max Autocorrelation Factors for Multivariate Spatial Imagery. Technical Report 6, Department of Statistics, Stanford University, California, 10 p.

TECK COMINCO LIMITED, 2003. Teck Cominco Limited 2002 Annual Report. Retrieved April 2003 from http://www.teckcominco.com/investors/reports/ar2002/tc-2002-operations.pdf.

XU, W., TRAN, T.T., SRIVASTAVA, R.M., and JOURNEL, A.G., 1992. Integrating seismic data in reservoir modelling: the collocated cokriging alternative. Proceedings, 67th Annual Technical Conference and Exhibition. Society of Petroleum Engineers, SPE paper No. 24742, p. 833-842.

WACKERNAGEL, H., 1995. Multivariate Geostatistics. Springer-Verlag, Berlin, 291 p.

ZHU, H. and JOURNEL, A.G., 1993. Formatting and integrating soft data: Stochastic imaging via the Markov-Bayes algorithm. *In* Geostatistics Troia '92, Volume 1. *Edited by* A. Soares. Kluwer Academic Publishers, Holland, p. 1-12.